Genes & Diseases (2022) 9, 1650–1661

Available online at www.sciencedirect.com

ScienceDirect

journal homepage: http://ees.elsevier.com/gendis/default.asp

FULL LENGTH ARTICLE

PGRN exacerbates the progression of non-small cell lung cancer via PI3K/AKT/Bcl-2 antiapoptotic signaling

Sicheng Chen [a], Mengjun Bie [a], Xiaowen Wang [a], Mengtian Fan [b], Bin Chen [b], Qiong Shi [b], Yingjiu Jiang [a,*]

[a] *Department of Cardiothoracic Surgery, The First Affiliated Hospital of Chongqing Medical University, Chongqing 400016, PR China*
[b] *Ministry of Education Key Laboratory of Diagnostic Medicine, School of Laboratory Medicine, Chongqing Medical University, Chongqing 400016, PR China*

Received 21 February 2021; received in revised form 25 May 2021; accepted 26 May 2021
Available online 1 July 2021

KEYWORDS
Bcl-2;
Cell apoptosis;
NSCLC;
PGRN;
PI3K/Akt

Abstract Progranulin (PGRN) is a growth factor that is involved in the progression of multiple tumors. However, the effects and molecular mechanisms by which PGRN induces lung cancer remain unclear. The expression level of PGRN was analyzed by conducting immunohistochemistry of the histological sections of lung tissues from non-small-cell lung carcinoma (NSCLC) patients. The proliferation, apoptosis, migration, and invasion of NSCLC cells were assessed by the MTT assay, Western blot, degree of wound healing, and Transwell assays. A nude mouse xenograft model was used to validate the role of PGRN *in vivo*. The expression level of PGRN was higher in male patients with lung adenocarcinoma than in those with lung squamous cell carcinoma; by contrast, no difference was observed in female patients. The overexpression of PGRN promoted the proliferation and anti-apoptosis of H520 (derived from lung squamous cell carcinoma) cells, whereas knockdown of PGRN inhibited the proliferation and anti-apoptosis of A549 (derived from lung adenocarcinoma) cells. Copanlisib (targeting PI3K) inhibited the increase in the expression of cell anti-apoptosis marker Bcl-2 induced by rhPGRN protein; the PI3K agonist 740 Y–P partially reversed the decrease in Bcl-2 expression induced by PGRN deficiency in both A549 and H520 cells. PGRN increased the expression of Ki-67, PCNA, and Bcl-2 *in vivo*. PGRN inhibited cell apoptosis depending on the PI3K/Akt/Bcl-2 signaling axis; PGRN positivity correlated with lung adenocarcinoma. PGRN is a potential biomarker for the treatment and diagnosis of NSCLC, especially in lung adenocarcinoma.

Abbreviations: MTT, 3-(4,5-dimethyl-2-thiazolyl)-2,5-diphenyl-2-H-tetrazolium bromide; NSCLC, Non-small cell lung cancer; Ad, Adenovirus; FBS, Fetal Bovine Serum; PBS, phosphate buffer saline; DMSO, Dimethyl sulfoxide; IHC, immunohistochemistry.

* Corresponding author. Department of Cardiothoracic Surgery, The First Affiliated Hospital of Chongqing Medical University, No. 1 Youyi Road, Yuzhong District, Chongqing 400016, PR China. Fax: +86 023 63310999.
E-mail address: jiangyinjiu@hospital.cqmu.edu.cn (Y. Jiang).
Peer review under responsibility of Chongqing Medical University.

https://doi.org/10.1016/j.gendis.2021.05.005

Introduction

Lung cancer, which causes approximately 1.6 million deaths every year, has become the leading cause of cancer-related deaths worldwide.[1] Non-small cell lung cancer (NSCLC) accounts for 85% in lung cancer cases.[2] Due to the lack of disease-associated symptoms, most patients first diagnosed with NSCLC have already progressed to an advanced stage and have a low 5-year survival rate.[3] Exploring novel molecular targets for the treatment and diagnosis of this condition will improve the 5-year survival rate and quality of life of patients with NSCLC.

Progranulin (PGRN) is a secreted growth factor with high glycosylation[4] and is involved in multiple biological processes in the human body, including early embryogenesis,[5] neurodegenerative,[6] tissue healing,[7] inflammation and host defense,[8] cartilage development and degradation.[9] PGRN regulates the proliferation, invasion, and metastasis of tumor cells.[10,11] Progranulin has become a prognostic indicator and treatment target for a variety of tumors.[12–17] In colorectal cancer, the transcriptional activity of PGRN can be regulated by lncRNA H19, miR-29b, and combined with the Wnt signaling pathway to promote endothelial–mesenchymal transition.[18] PGRN also increases the phosphorylation of Akt and Erk to promote the proliferation and angiogenesis of tumors.[19,20] In cholangiocarcinoma, progranulin regulates cell proliferation, apoptosis and invasion through PI3K/Akt pathway.[21] In bladder cancer, PGRN regulates the remodeling of the actin cytoskeleton by interacting with the actin-binding protein drebrin, which regulates tumor growth and promotes tumor cell movement and invasion.[22] As a potential interacting factor of PSCA, PGRN enhances the adhesion of prostate cancer cells to BMEC through the NF-κB/integrin-α4 pathway to promote the metastasis of prostate cancer.[23] PGRN also promoted the PD-L1 expression in tumor-associated macrophages (TAMs), which helps tumor cells to escape the immune system against $CD8^+$ T cells.[24] Another study demonstrated that PGRN promotes the progression of melanoma by inhibiting the recruitment of natural killer cells to the tumor microenvironment.[25] Yue et al[26] demonstrated that PGRN enhances MiR-5100 expression in TAMs, and this inhibits the CXCL12/CXCR4 axis by decreasing the CXCL12 expression in breast cancer cells. Moreover, PGRN enhances unanchored cell growth and metastasis by upregulating the VEGF in breast cancer.[27] Nielsen et al[28] proved that metastasis-related macrophage-secreted PGRN transforms the resident hepatic stellate cell into myofibroblasts, which secrete periosteal protein, sustaining a fibrotic microenvironment necessary for tumor cell growth and metastasis. The expression of PGRN is not correlated with the progression of ovarian cancer, but high expression of PGRN correlates with a low overall survival rate in patients with advanced ovarian cancer.[29] As mentioned earlier, PGRN is widely involved in the tumorigenesis and development of epithelial tissue-derived tumors, including breast tumors, ovarian cancer, and colorectal carcinoma. Lung cancer with the highest global incidence is also an epithelial-derived tumor, but the role of PGRN in the development of lung cancer remains unclear.

Here, we demonstrated that PGRN expression was higher in male patients with lung adenocarcinoma than in those with lung squamous cell carcinoma. *In vivo* and *in vitro*, PGRN promoted tumor proliferation, migration, and invasion, and inhibited the apoptosis of NSCLC cells through the PI3K/Akt/Bcl-2 axis in both A549 and H520 cells. These results may provide a new approach for the diagnosis and treatment of lung cancer.

Materials and methods

Specimens and ethics

Tissue samples were collected from 120 lung cancer patients (male = 78, female = 42) admitted in the Department of Cardiothoracic of the First Affiliated Hospital of Chongqing Medical University from Jan 2017 to Dec 2019. Almost all patients (n = 119) were not treated with antitumor drugs until the specimens were collected. Prior to the collection of all tissue specimens, informed consent was obtained from each patient; the study was approved by the institutional ethics committee of the First Affiliated Hospital of Chongqing Medical University. Female patients were excluded because no significant difference was found.

Immunochemistry

Paraffin sections of tumor tissue were dewaxed, hydrated, and antigen repaired. The sections were then blocked with normal goat serum for 30 min, incubated with primary antibody at 4 °C overnight, and then analyzed using an immunohistochemistry (IHC) kit (Zsbio Technology, Beijing, China). Staining was performed under standardized conditions. The sections were counterstained with hematoxylin, fixed, and covered with glass. Semi-quantitative evaluation of positive staining was performed by two independent pathologists. The staining intensity of sections was rated as follows: +++, strong positive; ++, positive; +, weak positive; and −, negative. Meanwhile, the percentage of positively stained cells was rated as follows: +++: >75%; ++: 50%–74%; +: 25%–49%; and −: <25%. The PGRN expression level (evaluated based on the staining intensity and the percentage of positively stained cells) was scored as 5–6: strong positive; 3–4: positive; and 0–2: negative. The intensity of staining and the percentage of positively stained cells from negative to strong positive were rated as 0, 1, 2, and 3 points, respectively, and the PGRN expression

level (IHC SCORE) was determined by adding the two scores above.

Sankey diagram

The Sankey diagram was constructed with R software (https://www.r-project.org/, version 3.6.3) using R packages ggplot2 (https://ggplot2.tidyverse.org/) and ggalluvial (http://corybrunson.github.io/ggalluvial/). The width of each band is proportional to the number of patients.

A549 and H520 cell culture

The human normal bronchial epithelial cell line HBE, lung adenocarcinoma cell line A549, and human lung squamous carcinoma cell line H520 were obtained from the American Type Culture Collection (Manassas, VA, USA). A549 cells were cultured in Dulbecco's Modified Eagle Medium/Nutrient Mixture F-12 (DMEM/F12; Gibco, C11330500BT, USA), while H520 cells were cultured in RM1640 (Gibco, C11875500BT, USA) supplemented with 10% fetal bovine serum (FBS; Gibco, 10099-141, USA) and 1% penicillin/streptomycin (P/S) at 37 °C in a 5% CO_2 incubator. MEK inhibitor PD98059 5 μM (MCE, CAS no. 167869-21-8, USA), trametinib 5 nM (MCE, CAS no. 871700-17-3, USA), PI3K inhibitor LY294002 1 μM (MCE, CAS no. 154447-36-6, USA), and copanlisib 10 nM (MCE, CAS no.1032568-63-0, USA) were used to target the PI3K/Akt and MAPK/Erk pathways, and 740Y—P 30 μM (MCE, CAS no. 1236188-16-1, USA) was used to activate PI3K.

Recombinant adenovirus infection

The efficiency of adenovirus infection was observed through a fluorescence microscope. Recombinant adenoviruses were generated using AdEasy technology as described.[30] The siRNA target sites against the human GRN coding region were selected using Dharmacon's siDESIGN program, and the siRNA oligonucleotide pairs were cloned into the pSES adenoviral shuttle vector to generate recombinant adenoviruses. The recombinant adenovirus AdR-siPGRN and negative control AdR-scramble were infected with A549 cells with polybrene (CAS no. 28728-55-4, USA). The used medium was replaced with fresh medium after 8 h.

Plasmid transfection

The coding regions of human GRN were polymerase chain reaction amplified and cloned into a pCMV-Flag plasmid to construct a PGRN overexpression plasmid (PGR group), which was used as a negative control (NC group). The mixture of 1 μg/ml PGRN overexpression plasmid, 1 μl/ml Lipo2000 (Invitrogen, Cat. no. 11668019, California, USA), and 100 μl medium without FBS and penicillin-streptomycin was incubated at room temperature (RT) for 30 min, and then evenly added into the culture dish. The medium was changed to complete medium after 4—6 h. The same amount of negative control plasmid was used to construct the NC group.

siRNA transfection and human recombinant PGRN

The small interfering RNAs targeting PGRN were designed and produced by Ruibo Biotechnology Co., Ltd. A total of 200 μl of basal medium DMEM/F12 in a 1:1 mixture (Gibco, C11330500BT, USA) without P/S was incubated with 8 μl of Lipo2000 (Cat. no. 11668019, Invitrogen, California, USA) and 50 nM of si-PGRN (Guangzhou Ruibo Biological Technology Co., Ltd.) for 5 min. The above two substances were then mixed and added to the medium. Refreshed to medium containing FBS for 6 h. Human recombinant PGRN was purchased from Beijing Sino Biological Co., Ltd. Exactly 800 μg/ml of hrPGRN was added to the medium. The proteins were extracted 36—48 h after all the above treatments.

Western blot assay

Whole-cell lysates were prepared from A549 and H520 cells. The total protein (30 μg) was loaded in a 10% sodium dodecyl sulfate polyacrylamide gel. The proteins were separated by electrophoresis at cold temperatures and then transferred in polyvinylidene fluoride membranes. The membranes were blocked in 10% fat-free milk for 2 h at RT, followed by incubation with a primary antibody at 4 °C overnight (PGRN 1:1000, #AF2420, RD; p-Akt 1:1000, #4060, Cell Signaling Technology; Akt 1:1000, #4685, Cell Signaling Technology; p-Erk 1:1000, #4370, Cell Signaling Technology; Erk 1:1000, #4695, Cell Signaling Technology; PCNA 1:1000, #13110, Cell Signaling Technology; Bcl-2 1:1000, #15071, Cell Signaling Technology; Bax 1:1000, #5023, Cell Signaling Technology; and cyclin D1 1:1,000, #2978, Cell Signaling Technology). The sections were incubated with secondary antibodies (ZsBio Technology, Beijing, China) for 2 h at RT after the previous step. Finally, the blot was exposed to the Bio-Rad Chemi Doc XRS imaging system.

Wound healing assay

A549 and H520 cells were seeded in 100-mm dishes and cultured at 37 °C until the cell density reached 85—90% confluence. The cells were scratched using a small pipette tip and then cells washed at least three times. Photos were taken at 0 h and 48 h to calculate the wound healing rate (wound healing rate = [wound width at 0 h−wound width at 48 h]/wound width at 0 h).

Transwell assay

Cell migration assays were performed using a 6-well Transwell plate. Briefly, 1×10^5 cells were resuspended in 350 μl serum-free medium and seeded into the upper chamber. The 700 μl medium containing 10% FBS was added to the lower chamber as an attractant. After 24 h of incubation, the upper cells were removed with a cotton swab, and the lower cells were fixed with crystal violet for 20 min. The number of cells in the lower chambers was

counted. The procedure of Transwell migration was the same as that of Transwell invasion, except that no Matrigel was placed in the upper chamber.

Colony-forming assay

A total of 500 A549 or H520 cells were added to a six-well plate. After 14 days of incubation, the medium was removed, gently washed three times with PBS, and fixed with 4% paraformaldehyde. Then, 300 μL of crystal violet dye solution was added to the wells. The medium was stained for 30 min, washed with PBS at least three times, air-dried, and photographed.

MTT assay

Cell proliferation was assessed using the MTT assay. 1×10^4 cells were seeded on 96-well plates with or without siRNA and plasmid, and the cells were cultured for 24, 48, and 72 h. At the indicated time, 10 μL of MTT (5 mg/ml) was added to each well, and incubation was continued at 37 °C for 4 h. The medium was then removed, and 150 μl of dimethyl sulfoxide (DMSO) was added to dissolve the MTT-formamide crystals. The Thermo Scientific Multiskan FC microplate photometer was used to detect the absorbance of the liquid at a wavelength of 492 nm.

Animal experiment

Animal experiments were performed in accordance with the guidelines established by the Animal Care and Use Committee of the Chongqing Medical University Laboratory Animal Research. The 6-week-old male BALB/c nude mice were purchased from HFK Bioscience Co., Ltd (Beijing, China) and randomly divided into four groups (A549 siPGRN group, $n = 5$; A549 scramble group, $n = 5$; H520 PGRN group, $n = 5$; and H520 NC group, $n = 5$). A549 or H520 cells (5×10^6) were injected subcutaneously into the mice. The tumor volume was measured every week and calculated as $V = a \times b^2 \times \pi/6$, where "a" and "b" represent the largest and smallest tumor diameters, respectively. The mice were sacrificed after 14 days. The protein levels of PCNA, Bcl-2, and Ki-67 were detected through IHC.

Statistical analysis

All data in this study were analyzed using the SPSS 20.0 and GraphPad statistical software. The mean ± standard deviation measurement data are shown. A *t*-test was used to compare the two groups. The comparison between multiple groups was performed using one-way analysis of variance. The spearman correlation coefficient was used to evaluate

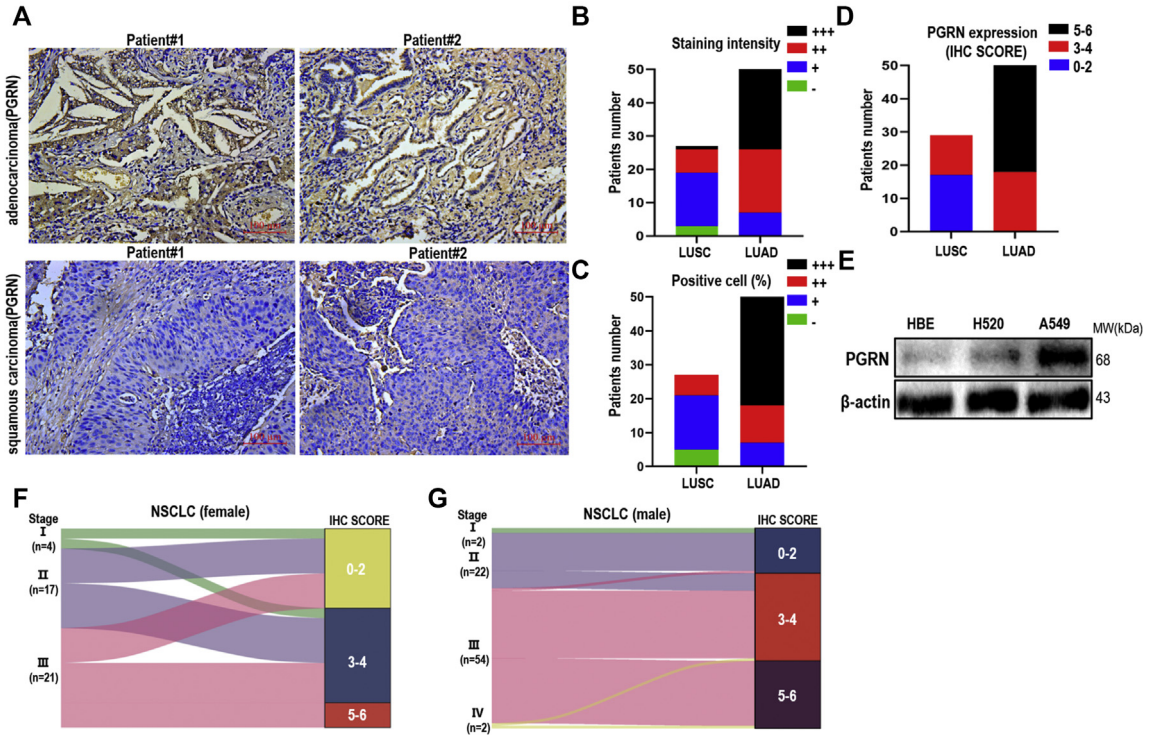

Figure 1 The expression level of PGRN in lung cancer tissues and lung cancer cell lines. **(A)** The expression of PGRN in lung squamous cell cancer and lung adenocarcinoma were detected by IHC. **(B)** Evaluation of immunohistochemistry staining intensity. **(C)** Assessment of the percentage of positively stained cell. **(D)** Comprehensive immunohistochemistry staining score. **(E)** The protein level of PGRN in HBE, H520 and A549 was analyzed by western blot. All experiments were repeated three times independently. **(F)** Mapping of IHC SCORE and clinical stage in female NSCLC (Sankey diagram, $P = 0.161$). **(G)** Mapping of IHC SCORE and clinical stage in male NSCLC (Sankey diagram, $P < 0.001$).

the correlation between immunohistochemistry and clinical stage. $P < 0.05$ was considered significant.

Results

Higher expression of PGRN in male patients with lung adenocarcinoma than in those with lung squamous cell carcinoma

To verify the expression of PGRN in lung cancer tissue samples, the patients' specimens were collected and subjected to IHC. The results showed that the expression of PGRN was higher in male patients with lung adenocarcinoma than in those with lung squamous cell carcinoma (27 with lung squamous cell carcinoma and 51 with lung adenocarcinoma, Fig. 1A and Table 1). Similar results were not observed in female patients (13 with lung squamous cell carcinoma and 29 with lung adenocarcinoma, Fig. 1F, G). To analyze the difference in immunochemistry staining between lung adenocarcinoma and lung squamous cell carcinoma, the staining intensity of PGRN and the percentage of positively stained cells in lung adenocarcinoma and lung squamous cell carcinoma specimens were strictly counted. Results showed that in the intensity (Fig. 1B) of PGRN staining and percentage of positively stained cells (Fig. 1C), the PGRN of lung squamous cell carcinoma specimens was significantly lower than that of lung adenocarcinoma specimens. The IHC SCORE based on the staining intensity and the percentage of positively stained cells of immunochemistry specimens also showed the same results (Fig. 1D). Compared with HBE cells, the PGRN expression levels were higher in A549 cells, whereas no difference was observed in H520 cells (Fig. 1E).

PGRN promoting proliferation, migration, and invasion in A549 and H520 cells

To investigate the effect of PGRN on A549 and H520 cells, the A549 cell line was selected to verify the phenotype of the decreased PGRN and H520 cell lines to verify the phenotype of PGRN overexpression. We decreased the PGRN expression using a specific siRNA in the A549 cells (Fig. 2A) and increased the PGRN expression using the PGRN overexpression vector in the H520 cells (Fig. 2B). The si-PGRN-treated A549 cells grew distinctly smaller than the NC group in the soft agarose medium (Fig. 2C). The PGRN-overexpressed H520 cells grew significantly faster than the NC group in the soft agarose medium (Fig. 2D). The proliferation rate of A549 cells treated with siPGRN was significantly lower than that of the scramble group (Fig. 2E). After the overexpression of PGRN, H520 cells showed stronger proliferation than the NC group (Fig. 2F). The A549 cells possessed a lower wound healing rate than the NC group at 48 h after decreasing the PGRN expression (Fig. 2G, H). By contrast, PGRN-overexpressed H520 cells showed a significantly higher wound healing rate than the NC group at 48 h (Fig. 2L, M). The migration assay with Transwells showed that the migration of A549 cells was inhibited compared with that of the control group after the knockdown of PGRN (Fig. 2I, J). The invasion assay with Matrigel-coated Transwells showed that the invasion of A549 cells was decreased compared with that of the control group after the knockdown of PGRN (Fig. 2I, K). The migration of H520 cells was evaluated compared with the control group after transfection with the PGRN overexpression plasmid (Fig. 2N, O). The invasion of H520 cells was not significantly different between the groups (Fig. 2N, P).

PGRN activating the MAPK/Erk and PI3K/Akt pathway in lung cancer cells

Western blotting was used to detect the phosphorylation level of Akt and Erk; results showed that the levels of p-Erk and p-Akt were significantly decreased in A549 cells compared with the control group after the knockdown of PGRN (Fig. 3A, B). Moreover, the levels of Cyclin D1, PCNA, and Bcl-2 were elevated in H520 cells overexpressing PGRN,

Table 1 Characteristic of patients.

Characteristic	Adenocarcinoma ($N = 80$)	Squamous carcinoma ($N = 40$)
Age — yr		
Mean	61.8 ± 10.9	61.4 ± 10.0
Median	58	61
Sex — no. (%)		
Female	29 (36)	13 (33)
Male	51 (64)	27 (67)
Smoking status — no. (%)		
Never smoked	37 (46)	5 (13)
Previous smoker	3 (4)	4 (10)
Current smoker	40 (50)	31 (78)
Current stage of disease — no. (%)		
I (Ia, Ib)	2 (3)	4 (10)
II (IIa, IIb)	22 (27)	16 (40)
III (IIIa, IIIb)	54 (67)	20 (50)
IV	2 (3)	0
Use of previous anticancer drug therapy — no. (%)	1 (1)	0

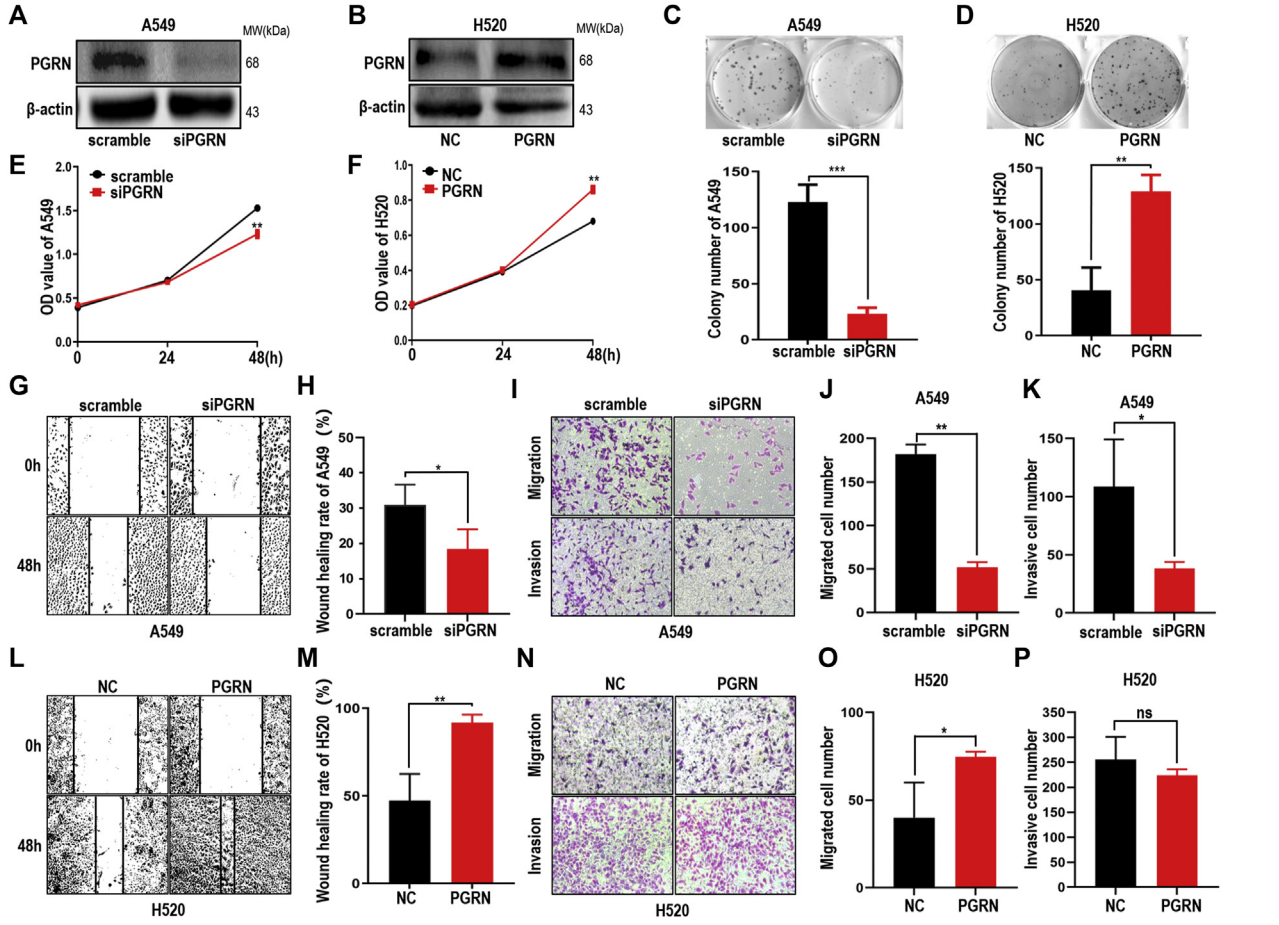

Figure 2 The effects of PGRN on proliferation, apoptosis, migration and invasion in A549 and H520. **(A)** The expression of PGRN was detected by western blot in A549 cells after knocking down PGRN. **(B)** The protein level of PGRN was detected by western blot in H520 cells after transfecting PGRN overexpression plasmid. **(C)** Colony number of A549 was detected by colony formation test after inhibiting PGRN (upper), and the quantitative statistics of colony number was shown (lower, $^{***}P < 0.001$ *vs*. Scramble group). **(D)** Colony number of H520 was detected by colony formation test after overexpressing PGRN (upper), and the quantitative statistics of colony number was shown (lower, $^{**}P < 0.005$ *vs*. Negative control group). **(E)** The proliferation ability of A549 was detected by MTT after knocking down PGRN ($^{**}P < 0.01$ *vs*. Scramble group). **(F)** The proliferation ability of H520 was detected by MTT after overexpressing PGRN ($^{**}P < 0.01$ *vs*. Negative control group). **(G)** The migration of A549 was detected by wound healing assay after knocking down PGRN. **(H)** The statistical graph was shown (right, $^{*}P < 0.05$ *vs*. scramble group). **(I)** The invasion and migration abilities of A549 were detected by transwell with or without matrix after knocking down PGRN. **(J, K)**. The statistical graph was shown ($^{*}P < 0.05$,$^{**}P < 0.01$ *vs*. scramble group). **(L)** The migration of H520 was detected by wound healing assay after overexpressing PGRN. **(M)** The statistical graph was shown ($^{**}P < 0.005$ *vs*. Negative control group). **(N)** The invasion and migration abilities of H520 were detected by transwell with or without matrix after overexpressing PGRN. **(O, P)** The statistical graph was shown ($^{*}P < 0.05$, P = ns *vs*. Negative control group). All experiments were repeated three times independently.

but that of Bax was decreased. Meanwhile, treatment of PGRN-overexpressed H520 cells with LY294002 or PD98059 reversed the expression of Cyclin D1, PCNA, Bcl-2, and Bax affected by PGRN (Fig. 3C—F). These results indicate that PGRN promotes tumor progression through the MAPK and PI3K/Akt signaling pathways.

PGRN/Akt/Bcl-2 axis regulating the apoptosis of NSCLC

To further clarify the specific mechanism by which PGRN regulates A549 and H520 cells, the antitumor drug copanlisib (PI3K) was used to explore the regulatory relationship between PGRN, Akt, and apoptosis-related Bcl-2 family proteins. In A549 cells, knockdown of PGRN with siRNA downregulated the phosphorylated Akt (p-Akt), PCNA, and Bcl-2 protein levels; this change was partially rescued by the PI3K agonist 740 Y—P. Meanwhile, the PI3K inhibitor copanlisib synergistically inhibited the downstream Bcl-2 with siPGRN (Fig. 4A—D). In H520 cells, the PGRN protein upregulated p-Akt and Bcl-2 (Fig. 4E, F). Similarly, this change can also be reversed by copanlisib; PI3K agonist 740 Y—P synergistically activates the downstream Bcl-2 with PGRN protein (Fig. 4E—H). These results indicate that PGRN protects against apoptosis by activating the downstream Akt and Bcl-2 cascade reactions.

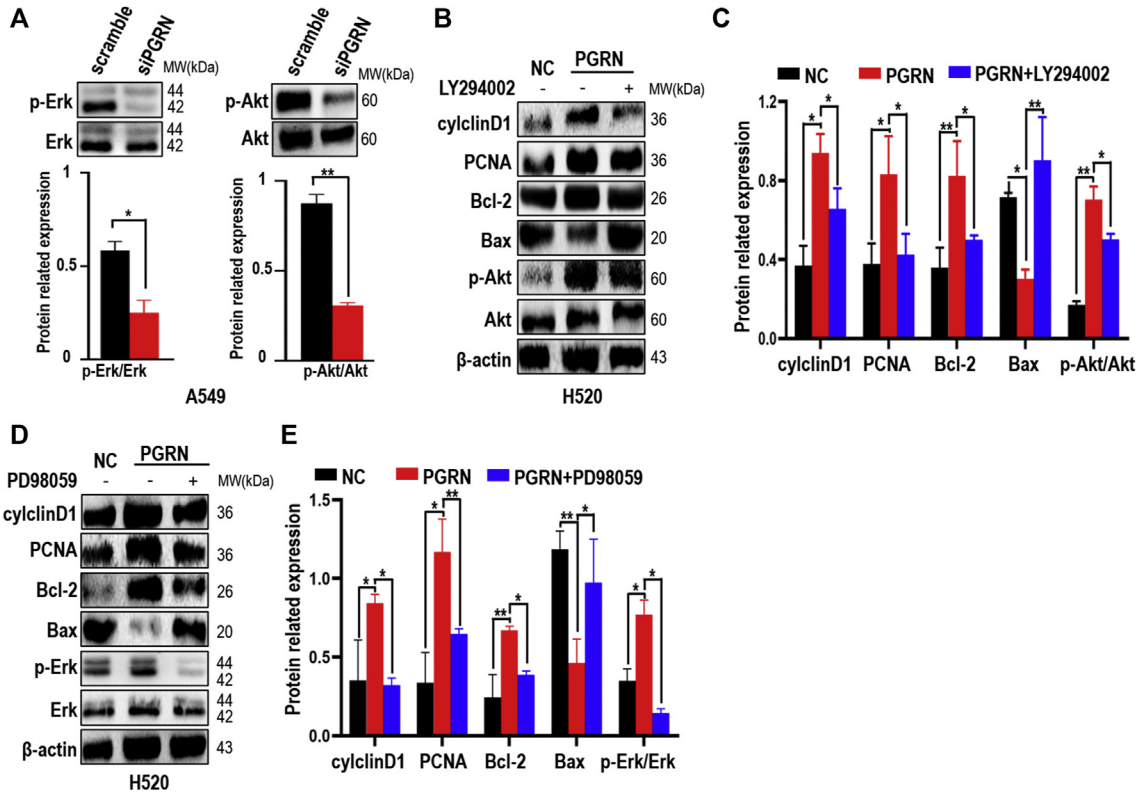

Figure 3 The signaling pathway of MAPK/Erk and PI3K/Akt underlying the effect of PGRN on lung cancer cells. **(A)** The protein levels of p-Erk, Erk, p-Akt and Akt in A549 were analyzed by western blot. **(B)** The quantitative statistics of protein expression was shown (*$P < 0.05$, **$P < 0.005$ *vs*. Scramble group). **(C)** The protein levels of CyclinD1, PCNA, Bcl-2, Bax, p-Erk, Erk, p-Akt and Akt in H520 after treating with LY294002 were analyzed by western blot. **(D)** The quantitative statistics of protein expression was shown (*$P < 0.05$, **$P < 0.005$ *vs*. Each another group). **(E)** The protein levels of CyclinD1, PCNA, Bcl-2, Bax, p-Erk, Erk, p-Akt and Akt in H520 after treating with PD98059 were analyzed by western blot. **(F)** The quantitative statistics of protein expression was shown (*$P < 0.05$, **$P < 0.005$ *vs*. Each another group). All experiments were repeated three times independently.

PGRN promoting the tumor progression *in vivo*

To demonstrate the effect of PGRN on lung cancer *in vivo*, A549 and H520 cells overexpressing PGRN were used to construct the xenograft model. The progression of xenograft tumors derived from PGRN-decreased A549 cells was significantly slower than that of the control group (Fig. 5A). The volume and weight of the PGRN-increased A549-derived tumors showed the same results (Fig. 5B, C). On the contrary, the overexpression of PGRN promoted the growth of H520-derived tumors compared with the NC group (Fig. 5D). The volume and weight of the tumors were also counted (Fig. 5E, F). The IHC of tumors showed that the expression of PCNA, Ki67, and Bcl-2 was downregulated in A549-derived tumors by knockdown of PGRN (Fig. 5G), while the expression of PCNA, Ki67, and Bcl-2 was upregulated in H520-derived tumors by the overexpression of PGRN (Fig. 5G). The above evidence supports the role of PGRN in promoting tumor progression *in vivo*.

Discussion

Here, we demonstrated that lung adenocarcinoma expressed higher levels of PGRN than squamous cell carcinoma. *In vitro*, the overexpression of PGRN enhances malignant biological behaviors such as proliferation, anti-apoptosis, migration, and invasion of NSCLC cell lines. This finding increases the possibility that PGRN can be used as a prognostic indicator for lung cancer. Mechanistically, this study revealed that PGRN regulates the expression of Bcl-2 through the classical PI3K/Akt pathway.

No difference was observed in the PGRN expression among the different pathological types of lung cancer in female patients. Serrero et al[31] reported that higher PGRN levels in the serum and tissue indicate a lower rate of survival in NSCLC patients. In view of the large gap in the incidence of different pathological types of lung cancer between men and women,[32,33] we paid attention to the possible differences in PGRN that indicated the advanced stage of NSCLC in men and women. In general, the expression level of PGRN in tissues can indicate a tumor malignancy. Because of the significant difference in the number of specimens from male and female patients, the expression level of PGRN in NSCLC is more representative of lung cancer in male patients, which will result in the concealment of the characteristics of female patients. Therefore, we conducted a statistic analysis on the two sexes. We found that, especially in male patients, PGRN levels had important clinical significance. We

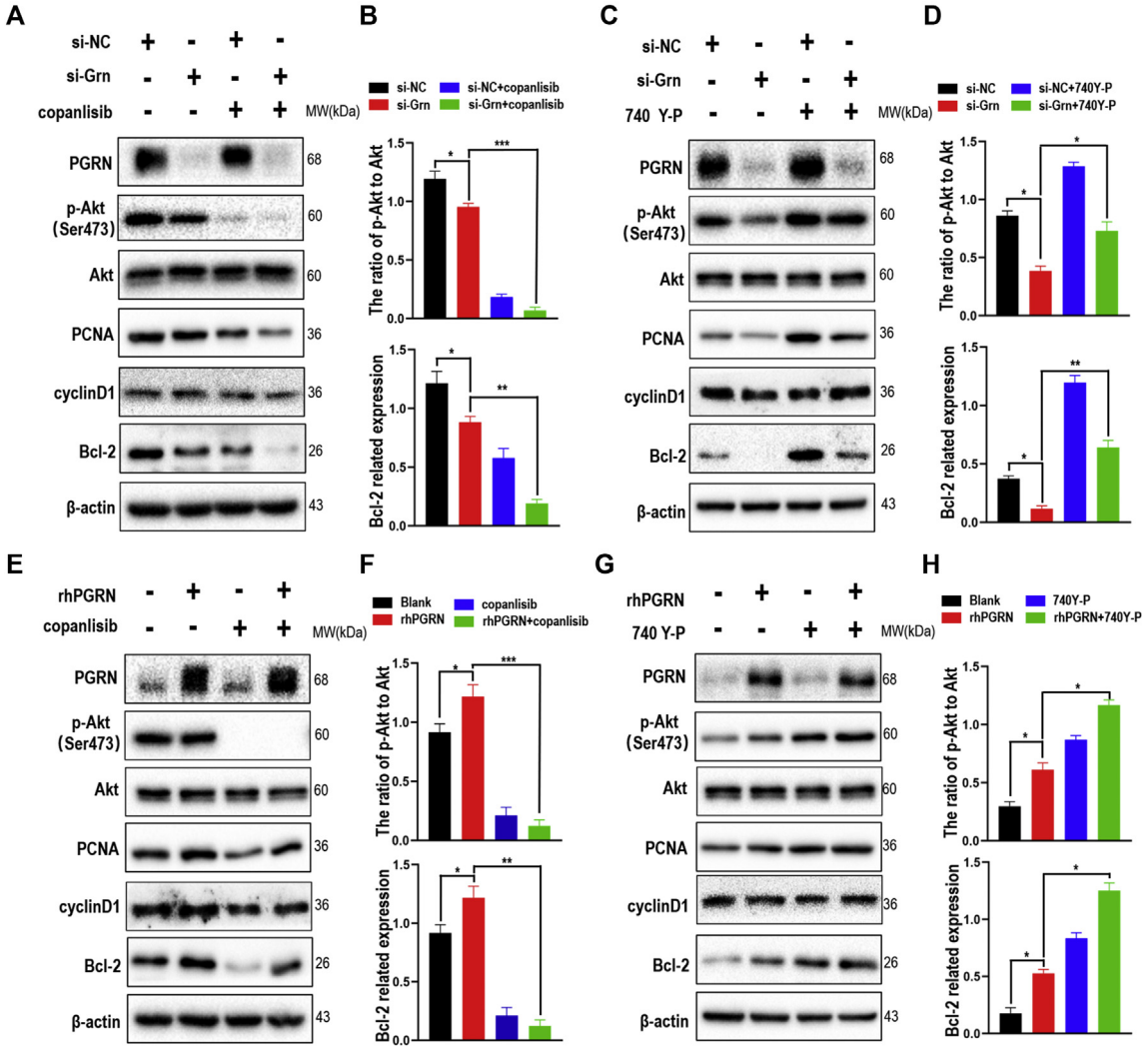

Figure 4 PGRN regulates cell apoptosis through AKT/Bcl-2 on A549 and H520 cell lines. **(A)** The protein levels of PGRN, p-Akt, Akt, CyclinD1, PCNA and Bcl-2 in A549 after treating with si-Grn and Copanlisib separately or together were analyzed by western blot. **(B)** The quantitative statistics of the ratio of p-Akt to Akt and the Bcl-2 expression was shown (*$P < 0.05$, **$P < 0.005$, ***$P < 0.001$). **(C)** The protein levels of PGRN, p-Akt, Akt, CyclinD1, PCNA and Bcl-2 in A549 after treating with si-Grn and 740 Y—P separately or together were analyzed by western blot. **(D)** The quantitative statistics of the ratio of p-Akt to Akt and the Bcl-2 expression was shown (*$P < 0.05$, **$P < 0.005$). **(E)** The protein levels of PGRN, p-Akt, Akt, CyclinD1, PCNA and Bcl-2 in H520 after treating with rhPGRN and Copanlisib separately or together were analyzed by western blot. **(F)** The quantitative statistics of the ratio of p-Akt to Akt and the Bcl-2 expression was shown (*$P < 0.05$, **$P < 0.005$, ***$P < 0.001$). **(G)** The protein levels of PGRN, p-Akt, Akt, CyclinD1, PCNA and Bcl-2 in H520 after treating with rhPGRN and 740 Y—P separately or together were analyzed by western blot. **(H)** The quantitative statistics of the ratio of p-Akt to Akt and the Bcl-2 expression was shown (*$P < 0.05$). All experiments were repeated three times independently.

demonstrated that PGRN promotes tumor proliferation, migration, and invasion, and inhibits apoptosis *in vitro*. This finding is consistent with the results of other studies on colon and ovarian cancer.[34,35] This may be related to the fact that they all originate from the mesoderm.[19,36–39] Based on the results of our experiment, as a classic pathway for tumor regulation,[40,41] the PI3K/Akt and MAPK/Erk signaling pathways are involved in the regulation of lung cancer cells through the expression of PGRN. Some studies have reported that PGRN is an upstream molecule that activates the downstream PI3K/Akt and MAPK signaling pathways in tumors.[20,21] Another study reported that inhibiting the PI3K/Akt and MAPK pathway activity induced the reduction of PGRN expression in ovarian clear cell carcinoma.[42] From our results, we found that the addition of hrPGRN promoted the expression of intracellular PGRN. The differences in the above research suggest that PGRN may form a self-feedback mechanism to regulate its expression through the PI3K/Akt and MAPK signaling pathways. The rapid endocytosis of PGRN, mediated by the lysosomal transporter sortilin, may also be another cause of the increase in the levels of endogenous progranulin.[43,44] Signal pathways are extremely complex regulatory networks, and crosstalk exists

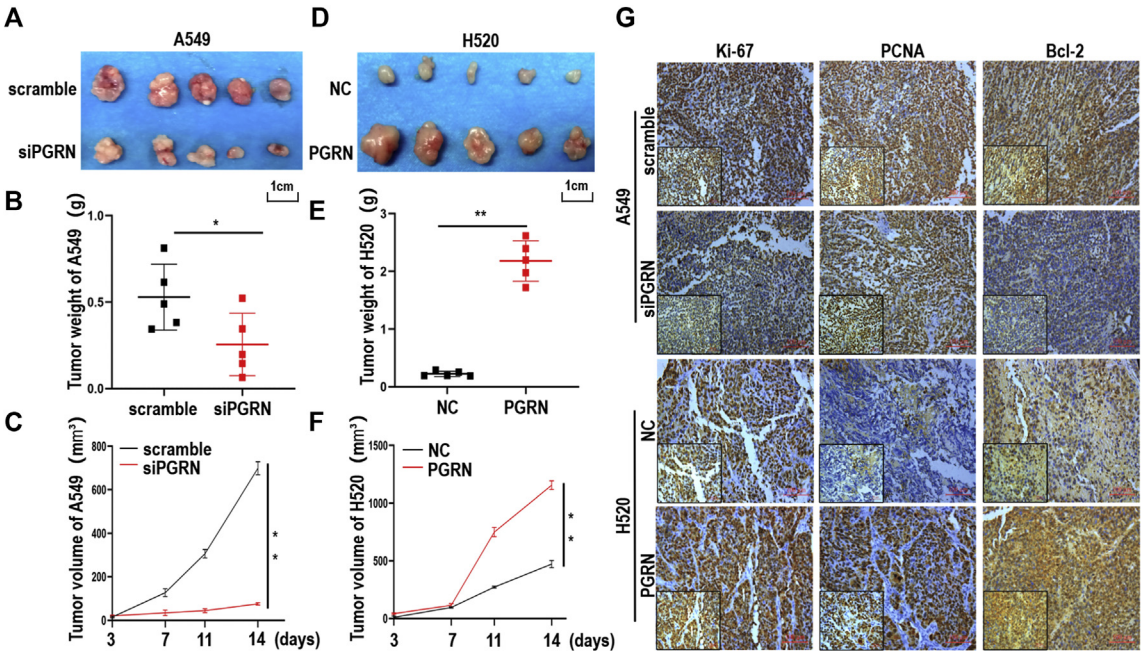

Figure 5 The effect of PGRN on A549 and H520 cells *in vivo*. **(A)** The A549 tumors were took out from nude mice 2 weeks after tumor implantation (siPGRN group: $n = 5$; scramble group: $n = 5$). **(B)** The statistical graph of tumor weight was shown (*$P < 0.05$ *vs*. scramble group). **(C)** The tumor growth curves were shown (**$P < 0.01$ *vs*. scramble group). **(D)** The H520 tumors were took out from nude mice 2 weeks after tumor implantation (PGRN group: $n = 5$; Negative control group: $n = 5$). **(E)** The statistical graph of tumor weight was shown (**$P < 0.05$ *vs*. Negative control group). **(F)** The tumor growth curves were shown (**$P < 0.01$ *vs*. Negative control group). **(G)** The expression of PCNA, Bcl-2 and Ki67 were detected by immunohistochemistry.

between them. Coupled with upstream effects and downstream negative feedback, it is difficult to fully explain the regulatory relationship between them.[45,46] It may be a more reliable strategy to reveal the determine the mechanisms of different tumor cell subtypes.

As a growth factor, PGRN exerts different biological functions in combination with different proteins. YB-1 exhibits immunomodulatory functions by affecting the binding of TNFα to its receptors; through its interaction with progranulin, YB-1 influences the TNFα-mediated signal transduction.[47] The mature secretory isoform of PGRN has been confirmed to be transported to the lysosome for cleavage by binding to SORT1.[48] More importantly, Neill et al reported that EphA2, as a functional receptor of progranulin, can be combined with progranulin to prolong the activation of the downstream Akt signaling pathway to promote capillary morphogenesis.[49] These evidences suggest that progranulin activates the downstream PI3K/Akt pathway in NSCLC and leads to anti-apoptosis is probably caused by the interaction with the functional receptor EphA2. Buraschi S et al proved that progranulin rather than ephrin-A1 (the canonical ligand of EphA2) is the main EphA2 ligand in bladder cancer. Progranulin causes Akt and Erk1/2-mediated phosphorylation of EphA2 on Ser897, which may drive bladder tumorigenesis. This suggests that the ligand of progranulin in tumors may be non-classical.[50] Exploring more PGRN receptors will better elucidate the specific mechanisms of tumor regulation. In future experiments, we will focus on PGRN receptors in tumors. Breaking the balance between proliferation and apoptosis is a typical characteristic of tumor cells.[51–54] Apoptosis is the maintenance of the stability of the internal environment and the autonomous and orderly death of cells controlled by genes and various cytokines. PI3K/Akt regulates apoptosis of the nasopharyngeal carcinoma cells.[55] PI3K/Akt-Bcl-2 acts as a classic signaling axis for regulating apoptosis.[56] Therefore, PGRN regulates Bcl-2 through the PI3K/Akt pathway, which is considered a strong evidence that PGRN promotes the growth of tumors. More cell lines will be included in future studies to demonstrate the universality of the mechanism in NSCLC and provide more reliable evidence. Meanwhile, more apoptosis indicators, such as the caspase family, p53 family, and survivin, will be tested. The nuclear translocation of NF-κB may also play an important role in apoptosis.[57] The in-depth mechanism by which PGRN regulates lung cancer apoptosis needs to be further explored. As a secreted protein, PGRN can be detected in the serum; in future research, we will further collect the serum of patients with lung cancer and analyze the relationship between PGRN in the serum and the lung cancer pathological index. This study provides an indicator for the early diagnosis and dynamic detection of lung cancer.

Drug resistance is one of the biggest obstacles to tumor treatment.[58–60] According to previous studies, PGRN is associated with tamoxifen resistance and poor prognosis in patients with breast cancer.[61] There may be some relationship between PGRN and drug resistance to guide clinical treatment and predict patient prognosis. However, the specific role and mechanism of PGRN in lung cancer resistance has not been reported in depth; hence, we will

further explore the relationship between PGRN and lung cancer drug resistance in future experiments.

Conclusion

According to publication and our findings, PGRN expression highly positive correlates with the malignant degree of non-small cell lung cancer in male patients, and PGRN regulates lung cancer cell apoptosis through the PI3K/Akt-Bcl-2 axis. These evidences further demonstrate the key role PGRN plays in tumor pathology and offer potential targets for non-small cell lung cancer treatment.

Author contributions

Conceptualization, CSC and JYJ; Methodology, CSC; Formal Analysis, CSC; Resources, FMT, CB and CSC; Data Curation, CSC and FMT; Writing — Original Draft Preparation, CSC; Writing — Review & Editing, JYJ; Visualization, JYJ.

Conflict of interests

The authors declare that they have no competing interests.

Funding

This research was supported by Chongqing Technology Innovation and application development special fund (No. cstc2019jscx-msxmX0095) and National Natural Science Foundation of China (No. NSFC 81672103). The authors are responsible for the results and opinions provided by this research, and the sponsor is not responsible for the content published.

Ethics declaration

The collection of clinical cancer patient specimens was approved by the Ethical Committee of the First Affiliated Hospital of Chongqing Medical University. All animal experiments strictly follow the guidelines of the Animal Experiment Center of Chongqing Medical University.

Acknowledgements

We are grateful to the scientific research staff of the Ministry of Education for key laboratory experiments in clinical laboratory diagnostics of the Medical College of Chongqing Medical University for their contributions to this study. We would like to thank Editage (www.editage.cn) for English language editing.

References

1. Bray F, Ferlay J, Soerjomataram I, Siegel RL, Torre LA, Jemal A. Global cancer statistics 2018: GLOBOCAN estimates of incidence and mortality worldwide for 36 cancers in 185 countries. *CA Cancer J Clin*. 2018;68(6):394—424.
2. Chen W, Zheng R, Zhang S, et al. Cancer incidence and mortality in China, 2013. *Cancer Lett*. 2017;401:63—71.
3. Hirsch FR, Scagliotti GV, Mulshine JL, et al. Lung cancer: current therapies and new targeted treatments. *Lancet*. 2017;389(10066):299—311.
4. Songsrirote K, Li Z, Ashford D, Bateman A, Thomas-Oates J. Development and application of mass spectrometric methods for the analysis of progranulin N-glycosylation. *J Proteomics*. 2010;73(8):1479—1490.
5. Cenik B, Sephton CF, Kutluk Cenik B, Herz J, Yu G. Progranulin: a proteolytically processed protein at the crossroads of inflammation and neurodegeneration. *J Biol Chem*. 2012;287(39):32298—32306.
6. Kao AW, McKay A, Singh PP, Brunet A, Huang EJ. Progranulin, lysosomal regulation and neurodegenerative disease. *Nat Rev Neurosci*. 2017;18(6):325—333.
7. Zhao YP, Tian QY, Frenkel S, Liu CJ. The promotion of bone healing by progranulin, a downstream molecule of BMP-2, through interacting with TNF/TNFR signaling. *Biomaterials*. 2013;34(27):6412—6421.
8. Yin F, Banerjee R, Thomas B, et al. Exaggerated inflammation, impaired host defense, and neuropathology in progranulin-deficient mice. *J Exp Med*. 2010;207(1):117—128.
9. Feng JQ, Guo FJ, Jiang BC, et al. Granulin epithelin precursor: a bone morphogenic protein 2-inducible growth factor that activates Erk1/2 signaling and JunB transcription factor in chondrogenesis. *FASEB J*. 2010;24(6):1879—1892.
10. Lu Y, Zheng L, Zhang W, et al. Growth factor progranulin contributes to cervical cancer cell proliferation and transformation in vivo and in vitro. *Gynecol Oncol*. 2014;134(2):364—371.
11. Wei Z, Huang Y, Xie N, Ma Q. Elevated expression of secreted autocrine growth factor progranulin increases cervical cancer growth. *Cell Biochem Biophys*. 2015;71(1):189—193.
12. Cui Y, Hettinghouse A, Liu CJ. Progranulin: a conductor of receptors orchestra, a chaperone of lysosomal enzymes and a therapeutic target for multiple diseases. *Cytokine Growth Factor Rev*. 2019;45:53—64.
13. Guha R, Yue B, Dong J, Banerjee A, Serrero G. Anti-progranulin/GP88 antibody AG01 inhibits triple negative breast cancer cell proliferation and migration. *Breast Cancer Res Treat*. 2021;186(3):637—653.
14. Göbel M, Eisele L, Möllmann M, et al. Progranulin is a novel independent predictor of disease progression and overall survival in chronic lymphocytic leukemia. *PLoS One*. 2013;8(8):e72107.
15. Do IG, Jung KU, Koo DH, et al. Clinicopathological characteristics and outcomes of gastrointestinal stromal tumors with high progranulin expression. *PLoS One*. 2021;16(1):e0245153.
16. Qin J, Huang S, Qian J, et al. The prognostic relevance and expression of progranulin in adult patients with acute myeloid leukemia. *Medicine (Baltimore)*. 2020;99(1):e18574.
17. Koo DH, Do IG, Oh S, et al. Prognostic value of progranulin in patients with colorectal cancer treated with curative resection. *Pathol Oncol Res*. 2020;26(1):397—404.
18. Ding D, Li C, Zhao T, Li D, Yang L, Zhang B. LncRNA H19/miR-29b-3p/PGRN Axis promoted epithelial-mesenchymal transition of colorectal cancer cells by acting on Wnt signaling. *Mol Cell*. 2018;41(5):423—435.
19. Yang D, Wang LL, Dong TT, et al. Progranulin promotes colorectal cancer proliferation and angiogenesis through TNFR2/Akt and ERK signaling pathways. *Am J Cancer Res*. 2015;5(10):3085—3097.
20. Yang D, Li R, Wang H, et al. Clinical implications of progranulin in gastric cancer and its regulation via a positive feedback loop involving AKT and ERK signaling pathways. *Mol Med Rep*. 2017;16(6):9685—9691.
21. Daya M, Loilome W, Techasen A, et al. Progranulin modulates cholangiocarcinoma cell proliferation, apoptosis, and motility via the PI3K/pAkt pathway. *Onco Targets Ther*. 2018;11:395—408.

22. Buraschi S, Neill T, Xu SQ, et al. Progranulin/EphA2 axis: a novel oncogenic mechanism in bladder cancer. *Matrix Biol*. 2020;93:10—24.
23. Zhao Z, Li E, Luo L, et al. A PSCA/PGRN-NF-κB-Integrin-α4 Axis promotes prostate cancer cell adhesion to bone marrow endothelium and enhances metastatic potential. *Mol Cancer Res*. 2020;18(3):501—513.
24. Fang W, Zhou T, Shi H, et al. Progranulin induces immune escape in breast cancer via up-regulating PD-L1 expression on tumor-associated macrophages (TAMs) and promoting CD8(+) T cell exclusion. *J Exp Clin Cancer Res*. 2021;40(1):4.
25. Voshtani R, Song M, Wang H, et al. Progranulin promotes melanoma progression by inhibiting natural killer cell recruitment to the tumor microenvironment. *Cancer Lett*. 2019;465:24—35.
26. Yue S, Ye X, Zhou T, et al. PGRN(-/-) TAMs-derived exosomes inhibit breast cancer cell invasion and migration and its mechanism exploration. *Life Sci*. 2021;264:118687.
27. Tangkeangsirisin W, Serrero G. PC cell-derived growth factor (PCDGF/GP88, progranulin) stimulates migration, invasiveness and VEGF expression in breast cancer cells. *Carcinogenesis*. 2004;25(9):1587—1592.
28. Nielsen SR, Quaranta V, Linford A, et al. Macrophage-secreted granulin supports pancreatic cancer metastasis by inducing liver fibrosis. *Nat Cell Biol*. 2016;18(5):549—560.
29. Carlson AM, Maurer MJ, Goergen KM, et al. Utility of progranulin and serum leukocyte protease inhibitor as diagnostic and prognostic biomarkers in ovarian cancer. *Cancer Epidemiol Biomarkers Prev*. 2013;22(10):1730—1735.
30. Luo J, Deng ZL, Luo X, et al. A protocol for rapid generation of recombinant adenoviruses using the AdEasy system. *Nat Protoc*. 2007;2(5):1236—1247.
31. Edelman MJ, Feliciano J, Yue B, et al. GP88 (progranulin): a novel tissue and circulating biomarker for non-small cell lung carcinoma. *Hum Pathol*. 2014;45(9):1893—1899.
32. Iams WT, Porter J, Horn L. Immunotherapeutic approaches for small-cell lung cancer. *Nat Rev Clin Oncol*. 2020;17(5):300—312.
33. Herbst RS, Morgensztern D, Boshoff C. The biology and management of non-small cell lung cancer. *Nature*. 2018;553(7689):446—454.
34. Chen XY, Li JS, Liang QP, He DZ, Zhao J. Expression of PC cell-derived growth factor and vascular endothelial growth factor in esophageal squamous cell carcinoma and their clinicopathologic significance. *Chin Med J (Engl)*. 2008;121(10):881—886.
35. Custodio A, Mendez M, Provencio M. Targeted therapies for advanced non-small-cell lung cancer: current status and future implications. *Cancer Treat Rev*. 2012;38(1):36—53.
36. Eguchi R, Nakano T, Wakabayashi I. Progranulin and granulin-like protein as novel VEGF-independent angiogenic factors derived from human mesothelioma cells. *Oncogene*. 2017;36(5):714—722.
37. He Z, Ong CH, Halper J, Bateman A. Progranulin is a mediator of the wound response. *Nat Med*. 2003;9(2):225—229.
38. Ichimura Y, Asano Y, Akamata K, et al. Progranulin overproduction Due to Fli-1 deficiency contributes to the resistance of dermal fibroblasts to tumor necrosis factor in systemic sclerosis. *Arthritis Rheumatol*. 2015;67(12):3245—3255.
39. Dong T, Yang D, Li R, et al. PGRN promotes migration and invasion of epithelial ovarian cancer cells through an epithelial mesenchymal transition program and the activation of cancer associated fibroblasts. *Exp Mol Pathol*. 2016;100(1):17—25.
40. Lavoie H, Gagnon J, Therrien M. ERK signalling: a master regulator of cell behaviour, life and fate. *Nat Rev Mol Cell Biol*. 2020;21(10):607—632.
41. Hoxhaj G, Manning BD. The PI3K-AKT network at the interface of oncogenic signalling and cancer metabolism. *Nat Rev Cancer*. 2020;20(2):74—88.
42. Perez-Juarez CE, Arechavaleta-Velasco F, Zeferino-Toquero M, Alvarez-Arellano L, Estrada-Moscoso I, Diaz-Cueto L. Inhibition of PI3K/AKT/mTOR and MAPK signaling pathways decreases progranulin expression in ovarian clear cell carcinoma (OCCC) cell line: a potential biomarker for therapy response to signaling pathway inhibitors. *Med Oncol*. 2019;37(1):4.
43. Hu F, Padukkavidana T, Vægter CB, et al. Sortilin-mediated endocytosis determines levels of the frontotemporal dementia protein, progranulin. *Neuron*. 2010;68(4):654—667.
44. Zheng Y, Brady OA, Meng PS, Mao Y, Hu F. C-terminus of progranulin interacts with the beta-propeller region of sortilin to regulate progranulin trafficking. *PLoS One*. 2011;6(6):e21023.
45. Wiegering A, Uthe FW, Jamieson T, et al. Targeting translation initiation bypasses signaling crosstalk mechanisms that maintain high MYC levels in colorectal cancer. *Cancer Discov*. 2015;5(7):768—781.
46. Zhu Z, Aref AR, Cohoon TJ, et al. Inhibition of KRAS-driven tumorigenicity by interruption of an autocrine cytokine circuit. *Cancer Discov*. 2014;4(4):452—465.
47. Hessman CL, Hildebrandt J, Shah A, et al. YB-1 Interferes with TNFα-TNFR binding and modulates progranulin-mediated inhibition of TNFα signaling. *Int J Mol Sci*. 2020;21(19):7076.
48. Miyakawa S, Sakuma H, Warude D, et al. Anti-sortilin1 antibody up-regulates progranulin via sortilin1 down-regulation. *Front Neurosci*. 2020;14:586107.
49. Neill T, Buraschi S, Goyal A, et al. EphA2 is a functional receptor for the growth factor progranulin. *J Cell Biol*. 2016;215(5):687—703.
50. Buraschi S, Neill T, Xu SQ, et al. Progranulin/EphA2 axis: a novel oncogenic mechanism in bladder cancer. *Matrix Biol*. 2020;93:10—24.
51. Carneiro BA, El-Deiry WS. Targeting apoptosis in cancer therapy. *Nat Rev Clin Oncol*. 2020;17(7):395—417.
52. Qi C, Wang X, Shen Z, et al. Anti-mitotic chemotherapeutics promote apoptosis through TL1A-activated death receptor 3 in cancer cells. *Cell Res*. 2018;28(5):544—555.
53. Roberti MP, Yonekura S, Duong CPM, et al. Chemotherapy-induced ileal crypt apoptosis and the ileal microbiome shape immunosurveillance and prognosis of proximal colon cancer. *Nat Med*. 2020;26(6):919—931.
54. Nakatsuka T, Tateishi K, Kato H, et al. Inhibition of histone methyltransferase G9a attenuates liver cancer initiation by sensitizing DNA-damaged hepatocytes to p53-induced apoptosis. *Cell Death Dis*. 2021;12(1):99.
55. Lin YT, Wang HC, Tsai MH, Su YY, Yang MY, Chien CY. Angiotensin II receptor blockers valsartan and losartan improve survival rate clinically and suppress tumor growth via apoptosis related to PI3K/AKT signaling in nasopharyngeal carcinoma. *Cancer*. 2021;127(10):1606—1619.
56. Hers I, Vincent EE, Tavaré JM. Akt signalling in health and disease. *Cell Signal*. 2011;23(10):1515—1527.
57. Jiang JX, Mikami K, Venugopal S, Li Y, Török NJ. Apoptotic body engulfment by hepatic stellate cells promotes their survival by the JAK/STAT and Akt/NF-kappaB-dependent pathways. *J Hepatol*. 2009;51(1):139—148.
58. Kozovska Z, Gabrisova V, Kucerova L. Colon cancer: cancer stem cells markers, drug resistance and treatment. *Biomed Pharmacother*. 2014;68(8):911—916.
59. Namee NM, O'Driscoll L. Extracellular vesicles and anti-cancer drug resistance. *Biochim Biophys Acta Rev Cancer*. 2018;1870(2):123—136.
60. Wang Y, Fang Z, Hong M, Yang D, Xie W. Long-noncoding RNAs (lncRNAs) in drug metabolism and disposition, implications in

cancer chemo-resistance. *Acta Pharm Sin B*. 2020;10(1):105—112.
61. Tangkeangsirisin W, Hayashi J, Serrero G. PC cell-derived growth factor mediates tamoxifen resistance and promotes tumor growth of human breast cancer cells. *Cancer Res*. 2004;64(5):1737—1743.